ORDEM DOS ENGENHEIROS
2018 ano de das alterações climáticas
INFORMAÇÃO GEOESPACIAL NA ERA 4.0 PARA UM PLANETA EM MUDANÇA
25 E 26 DE OUTUBRO DE 2018
IX CNCG
CONFERÊNCIA NACIONAL DE CARTOGRAFIA E GEODESIA

Addressing anomalies on grapevines leaves: comparing unsupervised clustering, classification-based neural networks and vegetation indices using RGB images

Jonáš HRUŠKA[1], Luís PÁDUA[2], Telmo ADÃO[1,2], Pedro MARQUES[1], Raul MORAIS[1,2], Emanuel PERES[1,2] and Joaquim João SOUSA[1,2]

[1]Engineering Department, School of Sciences and Technology, University of Trás-os-Montes e Alto Douro, 5000-801 Vila Real, Portugal
[2]INESC-TEC, 4200-465 Porto, Portugal

(jonash@utad.pt; luispadua@utad.pt; telmoadao@utad.pt; pedro.marques@utad.pt; rmorais@utad.pt; eperes@utad.pt; jjsousa@utad.pt)

Key words: Precision viticulture, Grapevines leaves, Anomalies detection, Machine learning, Digital image processing, Vegetation indices, K-mean clustering

Abstract: To detect inconsistencies in any type of data first it is necessary to define what is considered to be anomalous. Usually, elements with characteristics opposed to those reputed as normal of local and/or global neighbourhood elements in the dataset are deemed anomalies. Some spots in grapevines leaves can signal the existence of biotic or abiotic problems, which may negatively influence both yield and quality. Indeed, crop diseases are responsible for major economic losses in the agriculture worldwide. As such, their early detection and mitigation is key to make agricultural production more efficient and sustainable. Traditional techniques for diseases detection in viticulture are conducted by in-field visual inspection or through laboratory analysis. Even though these techniques can have good results, they are a very time-consuming and demanding process when considering agricultural fields with considerable dimension. A more efficient, cheap and quick alternative is by means of automatic processing. In this study, computer vision techniques using images from the visible portion of the electromagnetic spectrum, also designated RGB, were explored for this purpose. Even though information provided by RGB images is limited for specific applications, recent studies have shown that when the proper processing is used, they can be used to detect grapevines biophysical parameters spatial variability. A comparison between three automatic techniques - unsupervised K-means clustering, supervised artificial neural network detection and vegetation indices – is also presented. Results show that anomalies that can be detected in visible part of electromagnetic spectrum are well identifiable by using vegetation indices, however, when neural network is well trained it seem to have a great potential for addressing anomalies in grapevines leaves as well.

1. Introduction

The issue of anomaly detection in any kind of data can be defined as finding anomalous pattern characteristics as opposed to normal behavior of local or global neighborhood samples in a given dataset. Detection of those patterns can provide useful information because anomalies usually point out a specific condition. A survey about anomaly detection where anomalies were defined with associated challenges was carried out by Chandola *et.* al (2009). In agriculture, there are many attributes that influence crops' development and potential yield. Some, such as the weather, soil or topography are hard to control, but others, like diseases, which are responsible for major economic losses in the agriculture industry worldwide (Martinelli et al., 2015) can be managed. A disease or plant stress can be represented by anomalous spots on the plant. Several techniques are used for detecting those spots. Traditional techniques consist in in-field visual observation by an agronomist and laboratory tests (Riley, Williamson, & Maloy, 2002). Even though this technique can provide good results, it is suitable for small areas because it is very time consuming and demanding. For bigger areas, remote sensing (RS) platforms are widely used. Indeed, RS is nondestructive and can cover large areas in short time with an adequate precision. Factors that mostly determine the quality of RS outputs are the platform and coupled sensor. There are three main platforms: satellites, manned aircrafts and unmanned aerial vehicles (UAVs). Each one has its limitations and advantages, but their suitability depends on the application and on the sensor that is used (Pádua et al., 2017). Sensors using bands from the visible part of the electromagnetic spectrum, also designated RGB, are the most common sensors currently available. The sensors capture the visible part of the electromagnetic spectrum and thus only visible anomalies can be detected. When regarding diseases, if the anomaly is visible it usually means that the disease is in its middle or late stage of development (Lowe et al, 2017). However, treatments are the most effective on early detections (Savary, Ficke, Aubertot, & Hollier, 2012) because future spreading can be stopped and appropriate treatment can be applied. Therefore, having a crop consistently monitored can be very important to detect the first signs of a disease. Due to their flexibility, adjustable granularity and low operational costs, UAVs are the most suitable RS platform to accomplish the task.

Recent studies (Kalisperakis et al, 2015; Mathews & Jensen, 2013) have demonstrated that RGB images can be used for monitoring spatial variability of grapevine biophysical parameters. Nevertheless, for estimating those parameters, accurate and automated segmentation methods are required to extract relevant information (Poblete-Echeverría et al , 2017). In that study, a machine learning (ML) approach is used for addressing anomalies in grapevines leaves and is then compared to common k-means clustering and vegetation indices (VIs) using RGB bands. ML is lately widely applied to classification, predicting future values, discovering structures and anomaly detection in many applications. This trend is mainly caused by the availability of data and high computational power that exist. Both factors are mandatory for a successful implementation of this approach and when they are met, ML has proven its efficiency and great potential (Chlingaryan et al, 2018).

ML approach using RGB images in agriculture was used in Lameski *et.* al (2017) for weed detection, while in (Lottes et al, 2017) it allow to detect crops and classify weeds. (Debats et al, 2015) used a generalized computer vision approach using ML to map crop fields in agricultural landscapes and (Poblete-Echeverría et al., 2017) used ML, VIs and k-means clustering for segmentation of grapevines canopy. (Xue & Su, 2017) made a review of developments and applications of VIs, as they were used in many studies. K-means clustering is an unsupervised statistical classification method, popular for its relatively easy implementation. Related studies using K-means clustering are (Nair et al, 2016; Poblete-Echeverría et al, 2017; Tete & Kamlu, 2017).

2. Material and Methods

This section describes the used dataset and the methods used for anomalies detection.

2.1 Used imagery data

Five RGB images of grapevines leaves were used in this study, see **Erro! A origem da referência não foi encontrada.**. In the leaves are visible different levels of anomaly – inconsistent RGB values, presented by light green and brown color, which were used for creation of anomaly mask, see Figure 2. Different colors may represent different development stage of the anomaly, but this fact was not considered in this work. Leaves A., B and C, have almost no visible anomalies, while leaves D and E are the most affected. The RGB images were created by exporting adequate bands from hyperspectral data; 670,11 nm for red band, 540,57 nm for green band and 480,65 nm for blue band. The hyperspectral data were acquired by Nano-Hyperspec (uVS-320) sensor with 15 ms frame period, 15 ms exposure, spectral range from 400 to 1000 nm (VNIR) and 270 bands.

Figure 1 – Five RGB grapevines leaves images with different levels of visible anomalies

Reference masks were manually created to define the visible anomalous areas in each leaf, as presented in **Figure 2**. These masks were then used in the assessment of the performance of the methods evaluated in this study. While leaf A has 0.54% anomalies, leaf B has 0.88% and leaf C 0.58%. Leaves D and E are the most affected with 11.33% and 33.52%, respectively.

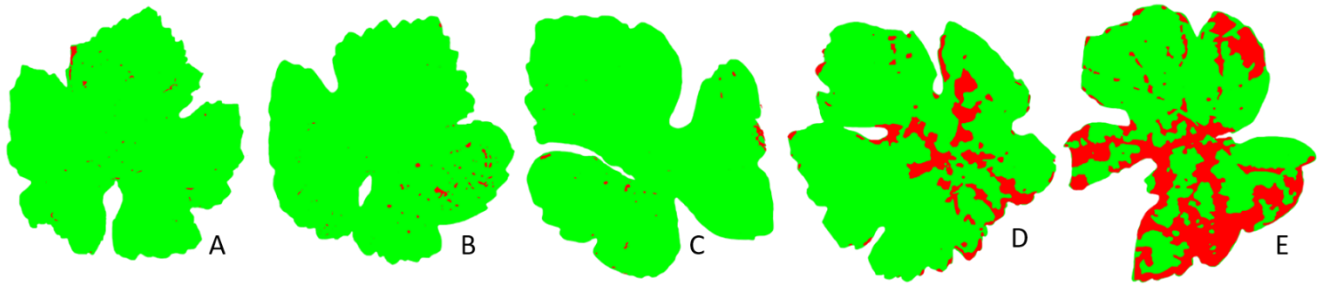

Figure 2 – Reference anomaly masks where green represents healthy portions and the color red visible anomalies of the grapevines leaves

2.2 Neural network classification

Neural network (NN) processing is inspired by the human brain functionality and uses generalization to learn regularities from training samples that transfer to new samples (Weigend et al , 1993). The network structure makes it possible to analyze complex dependencies among the dataset and thus solve problems that common statistical methods struggle with (Shafri, 2016). The network does not need to be explicitly programmed: parts of the NN structure are used like “black boxes” (Mitchell, 1997), which hides the complexity. Many parameters and the network structure are empirically modified.

NN structure used in this study is depicted in **Figure 3**, where three inputs can be seen in the respective layer as a value of RGB bands in the leaves’ images. One hidden layer with 10 neurons, followed by output layer with two outputs representing healthy portion “H” or the anomaly “A”.

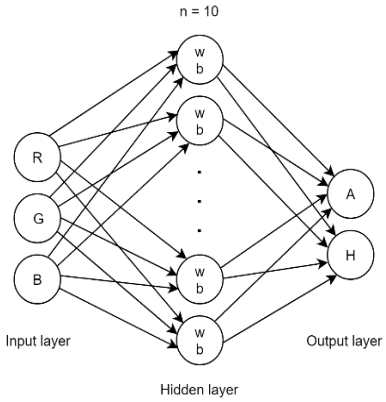

Figure 3 – Neural network structure used in this study to classify healthy and unhealthy portions of grapevines leaves RGB images

When using NN, several steps need to be ensured: The general workflow contains data acquisition, pre-processing - where data is cleaned and normalized -, followed by the building of the network structure and tuning the parameters. After the network structure is built, the training process can be conducted. The NN will learn inputs consistencies. In this study, a total of 1357 samples for training, randomly selected within the leaves, were used; 684 samples of grapevine leaves with healthy portions and 664 samples of anomalies. Exact numbers of the inputs can be seen in Table 1. Therefore, the trained NN was used for predictions. Acquired results should help in correcting the parameters configuration because of the gained insights about the dataset. The predictions for each pixel in the leaf with higher than 90 % certainty were binarized and compared against the reference anomaly masks (Figure 2). The binarization created black and white image with white color representing the predictions for anomalous parts. Last step was to appropriately visualize both data and results.

Table 1 – Number of healthy and anomalous training samples taken from the five grapevines leaves used in this study.

Leaf	A	B	C	D	E
Healthy	195	158	104	112	115
Anomaly	141	140	121	134	128

2.3 K-means clustering

Clustering is a method that groups similar unlabeled patterns into a number of clusters (Gordon et al., 1999). K-means clustering is a common unsupervised partitioning method used in image processing that produces a clustering for specified number of classes. First step in the calculation is initialization of K clusters with K centroids (one for each cluster). The clusters with the centroids are then recalculated until all the data in each cluster are at minimum distance from their centroids (Macqueen, 1967). The algorithm is widely used due to its simple implementation and generally fast outputs. The data were grouped into two clusters: healthy and anomalous portions and then outputs representing anomalies were selected and binarized and finally compared with reference anomaly masks (Figure 2).

2.4 Vegetation indices

VIs are used for quantitative and qualitative evaluation of vegetation cover, vigor and other applications (Xue & Su, 2017). For their calculation simple mathematical operations or the transformation of spectral bands are used. They can be divided into two groups according to the width of the bands they use: broadband or narrow band VIs (Agapiou et al , 2012). Another division can be based on the part of the electromagnetic spectrum from which the used bands are. In this study images from the visible part of the electromagnetic spectrum are used and thus only indices calculated with those bands were selected. The list of indices used, and the corresponding equations is presented in **Table 2**. Outputs of VIs were segmented by Otsu's thresholding method (Otsu, 1979). All binary results from each method were evaluated against the reference masks (Figure 2).

Table 2 – Used RGB vegetation indices, respective equations and references

Vegetation index	Equation	Reference
Green-Red Vegetation Index	$GRVI = (R_{green} - R_{red})/ (R_{green}+R_{red})$	(Tucker, 1979)
Modified Green-Red Vegetation Index	$MGRVI = (R_{green} - R_{red})^2/ (R_{green}+R_{red})^2$	(Bendig, 2015)
Blue/Green Pigment Index	$BGVI = (R_{blue} - R_{green})$	(Zarco-Tejada et al., 2005)
Blue/Red Pigment Index	$BRVI = (R_{blue} – R_{red})$	(Zarco-Tejada et al., 2005)
Excess Green	$ExG = (2*g_n – r_n - b_n)$	(Woebbecke et al., 1995)
Vegetativen	$VEG = (g_n)/(r_n\text{^}(a)* b_n\text{^}(1-a))$; where a = 0.667	(Hague et al., 2006)

Vegetation Index Green	$Varig = (R_{green} - R_{red})/(R_{green} - R_{red} - R_{blue})$	(Gitelson, et al., 2002)
Red-green-blue vegetation index	$RGBVI = ((R_{green})^2 - (R_{blue}*R_{red}))/((R_{green})^2 + (R_{blue}*R_{red}))$	(Bendig, 2015)
Triangular Greenness Index	$TGI = R_{green} - 0.39*R_{red} - 0.61*R_{blue}$	(Hunt et al., 2013)
2G_RGI	$2G\_RGI = 2*R_{green} - (R_{red} - R_{blue})$	(Richardson et al., 2007)
Green Percentage Index	**G%** $= (R_{green}) / (R_{red} + R_{green} + R_{bue})$	(Richardson et al., 2007)

where: $r_n = (R_{ed})/(R_{red}+R_{green}+R_{blue})$; $g_n = (R_{green})/(R_{red}+R_{green}+R_{blue})$; $b_n = (R_{blue})/(R_{red}+R_{green}+R_{blue})$

3. Results

To make the results more relevant for cases such as leaves A, B and C – where the visible anomalies are a small portion when compared with the healthy part - the binary images complement was used. Plus, the VIs are mostly designed for detection of healthy parts in vegetation. Complement images were created also from the anomaly reference masks. Results are presented in Tables 3, 4 and 5 with: percentage of correctly detected pixels (true positives – TP); pixels that were detected but should not have been, considered as over detection (false positives - FP); and pixels that were not detected, considered as under detection (false negatives - FN). Precision, sensitivity and false negative rate (FNR) were obtained from the following equations (Olson & Delen, 2008):

$$Precision = TP/(TP+FP) \quad (1)$$

$$Sensitivity = TP/(TP+FN) \quad (2)$$

$$FNR = 1-TP/(TP+FN)) \quad (3)$$

Precision is an expression of the statistical standard deviation, where it addresses how close are the estimates from different samples to each other. Sensitivity displays the ability of the technique to correctly detect pixels of interest and false negative rate is an indicator of how many pixels is predicted as not anomalous while they actually anomalous are. NN network results are presented in **Table 3**. The lowest proportion of correctly detected pixels is not below 90%. Leaf E – the most visibly affected by anomalies – had both the biggest over detection rate (2.65%) and under detection rate (8.83%), along with the lowest precision (97.17%) sensitivity (91.15%) and false negative rate (8.85%). The best precision was achieved with leaves A and B both with 99.96%.

Table 3 – Results obtained, per leaf, from NN method, for true positive classifications (TP), false positives (FP), false negatives (FN) and for precision, sensitivity and false negative rate (FNR), as well, the mean percentage value of all parameters

Leaves	TP (%)	FP (%)	FN (%)	Precision (%)	Sensitivity (%)	FNR (%)
A	95.76	0.04	4.20	99.96	95.80	4.20
B	95.18	0.04	4.78	99.96	95.22	4.78
C	96.76	0.05	3.19	99.95	96.81	3.19
D	92.94	0.80	6.26	99.15	93.69	6.31
E	90.93	2.65	8.83	97.17	91.15	8.85
Mean	94.31	0.72	5.45	99.24	94.53	5.47

Results of k-means clustering method are presented in **Table 4**. Most correctly detected pixels were achieved in leaf B with 74.01%, followed by leaf A, with 73.90%. Both of those leaves have in common a small proportion of visible anomalies. However, leaf C, with a similar proportion of anomalies, was achieved 50.94%, which is the lowest value.

Table 4 – Results obtained, per leaf, from K-means clustering method, for true positive classifications (TP), false positives (FP), false negatives (FN) and for precision, sensitivity and false negative rate (FNR), as well, the mean percentage value of all parameters

Leaves	TP (%)	FP (%)	FN (%)	Precision (%)	Sensitivity (%)	FNR (%)
A	73.90	0.24	25.86	99.68	74.08	25.92
B	74.01	0.82	25.17	98.90	74.62	25.38
C	50.94	0.28	48.78	99.45	51.08	48.92
D	64.46	9.31	26.23	87.38	71.08	28.92
E	54.53	21.01	24.46	72.19	69.03	30.97
Mean	63.57	6.33	30.10	91.52	67.98	32.02

In **Table 5** the results of VIs are presented. The overall best result was achieved by the Varig vegetation index with 97.04%, followed closely by GRVI with 96.97% and MGRVI with 96.83%. Nevertheless, GRVI achieved slightly lower over detection with 1,23% than the aforementioned VI. Lowest values were presented by TGI with 87.17% and 2G_RGI with 87.39%.

Table 5 – Mean values of the results obtained from vegetation indices computation, for true positive classifications (TP), false positives (FP), false negatives (FN), as well, the mean percentage value of the parameters

Vegetation index	TP (%)	FP (%)	FN (%)	Precision (%)	Sensitivity (%)	FNR (%)
GRVI	96.97	1.23	1.81	98.75	98.17	1.83
MGRVI	96.83	2.09	1.08	97.89	98.90	1.10
BGVI	89.45	9.30	1.26	90.58	98.61	1.39
BRVI	94.59	4.64	0.77	95.32	99.19	0.81
ExG	96.27	2.74	1.00	97.23	98.97	1.03
VEG	90.70	9.30	0.00	90.70	100	0
Varig	97.04	1.54	1.42	98.44	98.56	1.44
RGBVI	94.63	4.96	0.40	95.02	99.58	0.42
TGI	87.17	5.21	7.63	94.36	91.95	8.05
2G_RGI	87.39	4.48	8.13	95.12	91.49	8.51
G%	91.24	8.73	0.03	91.27	99.97	0.03

4. Conclusion

All tested techniques have been proven useful in addressing grapevines leaves anomalies detection, however with different performances. The best overall results were achieved by using VIs. Moreover, less effort is needed to determine them. NN had good results also, but with significantly more effort. K-means clustering using two clusters achieved the lowest performance.

It is important to be aware that only clearly visible symptoms were detected in this study and that in the field there are a lot of factors (e.g. pesticides, dust, weather conditions and others) that can influence the appearance of leaves. Those factors may make some spots look like anomalies, but with no significant importance to the plants' development, as opposed to diseases. Detection of anomalies that are more relevant for crops growth can be achieved by using sensors that capture a wider range of the electromagnetic spectrum, besides the visible part, namely hyperspectral sensors, but this study was focused on evaluation of image processing methods using the most accessible data to wide spectrum of user with the aim to find out their performances

for the task of automatic visible anomaly detection in grapevine leaves. The use of hyperspectral data for the same task will be conducted in future studies. Results of k-means clustering could be improved by using bigger number of "k" and each output compared with the reference mask and select the best cluster. VIs using narrower bands might reach even higher accuracies.

Acknowledgments

This work was financed by the European Regional Development Fund (ERDF) through the Operational Programme for Competitiveness and Internationalisation - COMPETE 2020 under the PORTUGAL 2020 Partnership Agreement, and through the Portuguese National Innovation Agency (ANI) as a part of project "PARRA - Plataforma integrAda de monitoRização e avaliação da doença da flavescência douRada na vinhA" (Nº 3447) and supported by the ERDF and North 2020 - North Regional Operational Program, as part of project "INNOVINEandWINE - Vineyard and Wine Innovation Platform" (NORTE–01–0145–FEDER–000038).

References

Agapiou, A., Hadjimitsis, D. G., & Alexakis, D. D. (2012). Evaluation of Broadband and Narrowband Vegetation Indices for the Identification of Archaeological Crop Marks. *Remote Sensing*, *4*(12), 3892–3919. https://doi.org/10.3390/rs4123892

Bendig, J. (2015). Unmanned aerial vehicles (UAVs) for multi-temporal crop surface modelling - A new method for plant height and biomass estimation based on RGB-imaging.

Chandola, V., Banerjee, A., & Kumar, V. (2009). Anomaly Detection: A Survey. *ACM Comput. Surv.*, *41*(3), 15:1–15:58. https://doi.org/10.1145/1541880.1541882

Chlingaryan, A., Sukkarieh, S., & Whelan, B. (2018). Machine learning approaches for crop yield prediction and nitrogen status estimation in precision agriculture: A review. *Computers and Electronics in Agriculture*, *151*, 61–69. https://doi.org/10.1016/j.compag.2018.05.012

Debats, S., Luo, D., Estes, L., Fuchs, T. J., & Caylor, K. K. (2015). A generalized computer vision approach to mapping crop fields in heterogeneous agricultural landscapes. https://doi.org/10.7287/peerj.preprints.1367v1

Gitelson, A. A., Kaufman, Y. J., Stark, R., & Rundquist, D. (2002). Novel algorithms for remote estimation of vegetation fraction. *Remote Sensing of Environment*, *80*(1), 76–87. https://doi.org/10.1016/S0034-4257(01)00289-9

Gordon, A., Keiding, N., Cox, D., Tong, H., Isham, V., Tibshirani, R., … Reid, N. (1999). *Classification, 2nd Edition*. Chapman and Hall/CRC. https://doi.org/10.1201/9781584888536

Hague, T., Tillett, N. D., & Wheeler, H. (2006). Automated Crop and Weed Monitoring in Widely Spaced Cereals. *Precision Agriculture*, *7*(1), 21–32. https://doi.org/10.1007/s11119-005-6787-1

Hunt, E. R., Doraiswamy, P. C., McMurtrey, J. E., Daughtry, C. S. T., Perry, E. M., & Akhmedov, B. (2013). A visible band index for remote sensing leaf chlorophyll content at the canopy scale. *International Journal of Applied Earth Observation and Geoinformation*, *21*, 103–112. https://doi.org/10.1016/j.jag.2012.07.020

Kalisperakis, I., Stentoumis, C., Grammatikopoulos, L., & Karantzalos, K. (2015). LEAF AREA INDEX ESTIMATION IN VINEYARDS FROM UAV HYPERSPECTRAL DATA, 2D IMAGE MOSAICS AND 3D CANOPY SURFACE MODELS. *ISPRS - International Archives of the Photogrammetry, Remote Sensing and Spatial Information Sciences*, *XL-1/W4*, 299–303. https://doi.org/10.5194/isprsarchives-XL-1-W4-299-2015

Lameski, P., Zdravevski, E., Trajkovik, V., & Kulakov, A. (2017). Weed Detection Dataset with RGB Images Taken Under Variable Light Conditions. In *ICT Innovations 2017* (pp. 112–119). Springer, Cham. https://doi.org/10.1007/978-3-319-67597-8_11

Lottes, P., Khanna, R., Pfeifer, J., Siegwart, R., & Stachniss, C. (2017). UAV-based crop and weed classification for smart farming. In *2017 IEEE International Conference on Robotics and Automation (ICRA)* (pp. 3024–3031). https://doi.org/10.1109/ICRA.2017.7989347

Lowe, A., Harrison, N., & French, A. P. (2017). Hyperspectral image analysis techniques for the detection and classification of the early onset of plant disease and stress. *Plant Methods*, *13*. https://doi.org/10.1186/s13007-017-0233-z

Macqueen, J. (1967). Some methods for classification and analysis of multivariate observations. In *In 5-th Berkeley Symposium on Mathematical Statistics and Probability* (pp. 281–297).

Martinelli, F., Scalenghe, R., Davino, S., Panno, S., Scuderi, G., Ruisi, P., … Dandekar, A. M. (2015). Advanced methods of plant disease detection. A review. *Agronomy for Sustainable Development*, *35*(1), 1–25. https://doi.org/10.1007/s13593-014-0246-1

Mathews, A. J., & Jensen, J. L. R. (2013). Visualizing and Quantifying Vineyard Canopy LAI Using an Unmanned Aerial Vehicle (UAV) Collected High Density Structure from Motion Point Cloud. *Remote Sensing*, *5*(5), 2164–2183. https://doi.org/10.3390/rs5052164

Mitchell, T. M. (1997). *Machine Learning* (1st ed.). New York, NY, USA: McGraw-Hill, Inc.

Nair, R. R., Adsul, S. S., Khabale, N. V., & Kawade, V. S. (2016). Analysis And Detection of Infected Fruit Part Using Improved k- means Clustering and Segmentation Techniques. *IOSR Journal of Computer Engineering*, 5.

Olson, D. L., & Delen, D. (2008). *Advanced data mining techniques*. Berlin: Springer.

Otsu, N. (1979). A TIreshold Selection Method from Gray-Level Histograms, 5.

Pádua, L., Vanko, J., Hruška, J., Adão, T., Sousa, J. J., Peres, E., & Morais, R. (2017). UAS, sensors, and data processing in agroforestry: a review towards practical applications. *International Journal of Remote Sensing*, *38*(8–10), 2349–2391. https://doi.org/10.1080/01431161.2017.1297548

Poblete-Echeverría, C., Olmedo, G. F., Ingram, B., & Bardeen, M. (2017). Detection and Segmentation of Vine Canopy in Ultra-High Spatial Resolution RGB Imagery Obtained from Unmanned Aerial Vehicle (UAV): A Case Study in a Commercial Vineyard. *Remote Sensing*, *9*(3), 268. https://doi.org/10.3390/rs9030268

Richardson, A. D., Jenkins, J. P., Braswell, B. H., Hollinger, D. Y., Ollinger, S. V., & Smith, M.-L. (2007). Use of digital webcam images to track spring green-up in a deciduous broadleaf forest. *Oecologia*, *152*(2), 323–334. https://doi.org/10.1007/s00442-006-0657-z

Riley, M. B., Williamson, M. R., & Maloy, O. (2002). American Phytopathological Society. Retrieved May 14, 2018, from https://www.apsnet.org/pages/default.aspx

Savary, S., Ficke, A., Aubertot, J.-N., & Hollier, C. (2012). Crop losses due to diseases and their implications for global food production losses and food security. *Food Security*, *4*(4), 519–537. https://doi.org/10.1007/s12571-012-0200-5

Shafri, H. Z. M. (2016). Machine Learning in Hyperspectral and Multispectral Remote Sensing Data Analysis. In *Artificial Intelligence Science and Technology* (Vols. 1–0, pp. 3–9). WORLD SCIENTIFIC. https://doi.org/10.1142/9789813206823_0001

Tete, T. N., & Kamlu, S. (2017). Detection of plant disease using threshold, k-mean cluster and ann algorithm. In *2017 2nd International Conference for Convergence in Technology (I2CT)* (pp. 523–526). https://doi.org/10.1109/I2CT.2017.8226184

Tucker, C. J. (1979). Red and photographic infrared linear combinations for monitoring vegetation. *Remote Sensing of Environment*, *8*(2), 127–150. https://doi.org/10.1016/0034-4257(79)90013-0

Weigend, A. S., Hertz, J. A., Krogh, A. S., & Palmer, R. G. (1993). *Review of John A. Hertz, Anders S. Krogh, and Richard G. Palmer, Introduction to the Theory of Neural Computation*.

Woebbecke, D. M. (University of N., Meyer, G. E., Von Bargen, K., & Mortensen, D. A. (1995). Color indices for weed identification under various soil, residue, and lighting conditions. *Transactions of the ASAE (USA)*. Retrieved from http://agris.fao.org/agris-search/search.do?recordID=US9561468

Xue, J., & Su, B. (2017). Significant Remote Sensing Vegetation Indices: A Review of Developments and Applications [Research article]. https://doi.org/10.1155/2017/1353691

Zarco-Tejada, P. J., Berjón, A., López-Lozano, R., Miller, J. R., Martín, P., Cachorro, V., … de Frutos, A. (2005). Assessing vineyard condition with hyperspectral indices: Leaf and canopy reflectance simulation in a row-structured discontinuous canopy. *Remote Sensing of Environment*, *99*(3), 271–287. https://doi.org/10.1016/j.rse.2005.09.002